

# Application of Zinc(II)–Binol for the Formal Aza-Diels–Alder Reaction of *N*-Arylimines with Danishefsky's Diene: CD-Based Absolute Stereochemistry Determination, Origin of Asymmetric Induction and Mechanistic Considerations

Lorenzo Di Bari,<sup>[a]</sup> Stéphane Guillarme,<sup>[b]</sup> John Hanan,<sup>[b]</sup> Andrew P. Henderson,<sup>[b]</sup> Judith A. K. Howard,<sup>[b]</sup> Gennaro Pescitelli,<sup>[a]</sup> Michael R. Probert,<sup>[b]</sup> Piero Salvadori,<sup>[a]</sup> and Andrew Whiting\*<sup>[b]</sup>

**Keywords:** Cycloaddition / Asymmetric catalysis / Configuration analysis / Nitrogen heterocycle / Lewis acid / Reaction mechanism

Zinc(II)–binol has been employed as an efficient Lewis acid catalyst (10 or 100 mol-% loading) for the formal aza-Diels–Alder reaction of ester, furyl and dimethyl acetal-substituted *N*-aryl imines. Asymmetric induction varies from poor to good, with the major enantiomer obtained being (*S*) when the (*S*)-binol complex has been employed. The absolute stereochemistry of the dimethyl acetal-substituted cycloadduct

was determined by CD, and both efficient aza-Diels–Alder reaction and asymmetric induction are proposed to be dependent upon the formation of bidentate zinc-imine complexes. These complexes have been modelled using semi-empirical methods.

(© Wiley-VCH Verlag GmbH & Co. KGaA, 69451 Weinheim, Germany, 2007)

## Introduction

Piperidine and indolizidine alkaloids occur widely in Nature and possess a range of biological activities,<sup>[1]</sup> with unnatural analogues in particular attracting much attention as therapeutic agents.<sup>[2]</sup> One method for accessing such six-membered aza-cycles has been the formal aza-Diels–Alder reaction,<sup>[3]</sup> and in recent years, there has been the development of catalytic asymmetric methods for producing asymmetric induction in the construction of such reactions.<sup>[3a,4]</sup> The most commonly used strategy for producing asymmetric induction of aza-Diels–Alder reactions is to employ a chiral Lewis acid to activate an imino-dienophile, which has resulted in several efficient asymmetric processes in recent years.<sup>[5]</sup> This is also a strategy which we have followed, having developed novel asymmetric catalytic methods to aza-Diels–Alder adducts derived from electron-deficient *N*-aryl imines, however, these methods proved difficult to reproduce and scale up.<sup>[6]</sup> This prompted us to develop robust catalytic asymmetric methods which: (1) employed a readily available catalytic system; (2) were easily reproducible; and

(3) could be potentially amenable to scale up. Hence, noting the application of zinc(II)–binol as an efficient asymmetric catalyst for both all-carbon Diels–Alder reactions<sup>[7]</sup> and aldehyde-dienophile hetero-Diels–Alder reactions,<sup>[8]</sup> we decided to examine the effect of this and closely related catalyst systems on imino-dienophile aza-Diels–Alder reactions, which resulted in an efficient catalytic asymmetric process based on the zinc(II)–binol system.<sup>[9]</sup> In this paper, we report our detailed work in this area, proposing the origin of the asymmetric induction, and our attempts to apply such methodology to different *N*-aryl imino dienophiles reacting with Danishefsky's diene<sup>[10]</sup> by a formal aza-Diels–Alder processes.<sup>[11]</sup>

## Results and Discussion

### Racemic Cycloadduct Formation

Several *N*-*p*-methoxyphenylimines **1** were prepared using literature methods.<sup>[12]</sup> The imines **1** were transformed into racemic formal Diels–Alder adducts using literature methods<sup>[9,13]</sup> with the exception of imines **1f** and **1g** which were treated with Danishefsky's diene **2**<sup>[10]</sup> using either magnesium(II) iodide or ytterbium(III) triflate as Lewis acid catalyst [Equation (1)] to give adducts **3f** and **3g** (Table 1). Furyl imine cycloadduct **3f** was found to readily crystallise to provide crystals which were suitable for single-crystal X-ray analysis (Figure 1). The N(1) atom has planar-trigonal geometry, and there is  $\pi$ -electron delocalisation along the

[a] Dipartimento di Chimica e Chimica Industriale, Via Risorgimento 35, 56126 Pisa, Italy

[b] Department of Chemistry, Durham University, Sciences Laboratories, South Road, Durham DH1 3LE, United Kingdom  
Fax: +44-191-384-4737  
E-mail: andy.whiting@durham.ac.uk

Supporting information for this article is available on the WWW under <http://www.eurjoc.org> or from the author.

practically planar N(1)C(8)=C(9)C(10)=O(2) moiety, which forms a dihedral angle of 38° with the benzene ring. The dihydropyridine ring adopts a twist conformation with the furanyl substituent in an axial orientation. The molecular conformation is similar to that of the 6-azetidine derivative.<sup>[14]</sup>

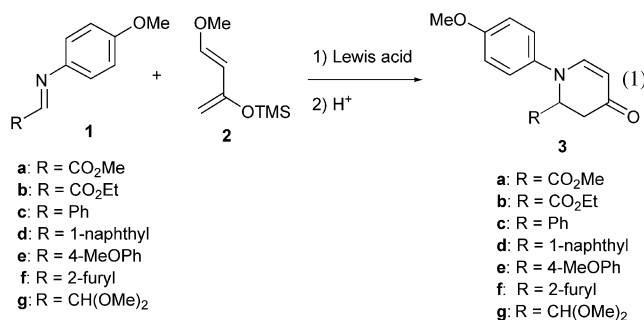


Table 1. Reaction of the imines **1f** and **g** with Danishefsky's diene **2**.

Entry	Cycloadduct	Catalyst	Solvent	Time [h]	% Yield <sup>[a]</sup> of <b>3</b>
1	<b>1f</b>	Yb(OTf) <sub>3</sub>	MeCN	18	76
2	<b>1g</b>	MgI <sub>2</sub>	MeCN	48	84

[a] Isolated yield after silica gel chromatography.

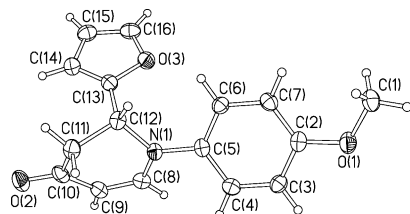


Figure 1. X-ray structure of the cycloadduct **3f** (50% thermal ellipsoids).

## Zinc(II)–Binol Catalysed Cycloadditions

With a range of different imines **1** in hand, reaction with Danishefsky's diene **2** in the presence of zinc(II)–binol was examined, as outlined by Equation (1); the corresponding results are shown in Table 2.

The reactions of the more electron-deficient imines **1a** and **b** show unexpected time, temperature and solvent effects, as discussed elsewhere,<sup>[9]</sup> however, it is possible to obtain reasonably high asymmetric induction with 100 mol-% of zinc(II)–binol and by carrying out the reaction in dichloromethane (Table 2, Entries 3 and 5). Under catalytic conditions (10 mol-%) and with a less polar solvent, asymmetric induction is only moderate to good, (Entries 1, 2 and 4). Comparing these results with a series of different imines **1c–g** was expected to show similar trends, however, the aryl imines **1c–f** had very poor reactivity towards Danishefsky's diene **2**, even with stoichiometric zinc(II)–binol catalyst. Indeed, the phenyl and 4-methoxyphenyl systems **1c** and **e**, respectively, were completely unreactive (Table 2, Entries 6 and 8). The naphthyl imine system **1d** also proved highly unreactive, with only 11% yield after a long (72 h) reaction time (Entry 7) when using stoichiometric zinc(II)–binol. With these results in hand, the furyl imine **1f** was expected to be even less reactive and indeed, this was the case in toluene (Entry 10). However, in dichloromethane, the imine **1f** was converted into the adduct **3f** albeit in a low (14%) yield (Entry 9). Even more odd was the reaction of dimethyl acetal imine system **1g**. Although the system was unreactive under catalytic zinc(II)–binol conditions (Entry 11, Table 2), it showed much higher reactivity than expected with the stoichiometric chiral Lewis acid, i.e. 59% yield of adduct **3g** after 18 h in toluene at room temperature, and a moderate (67%) *ee* (Entry 12, Table 2). On the basis of the CD curve and DFT calculations (*vide infra*), the absolute stereochemistry of this adduct, shown in Entry 12 (Table 2), was determined to be (*R*) [(*R*)-binol was used to prepare the

Table 2. Results for the zinc(II)–binol-catalysed aza-Diels–Alder reaction of imines **1** with Danishefsky's diene **2**.

Entry	Cycloadduct <b>3</b> R	Catalyst loading mol-% (absol. stereochem.)	Solvent	Temp. [°C]	Time [h]	% Yield <sup>[a]</sup> of <b>3</b>	% <i>ee</i> <sup>[b]</sup> (absol. stereochem.)
1	<b>a</b> CO <sub>2</sub> Me	100 ( <i>S</i> )	toluene	25	2.5	69	80 ( <i>S</i> ) <sup>[c]</sup>
2	<b>a</b> CO <sub>2</sub> Me	10 ( <i>S</i> )	toluene	25	15	68	56 ( <i>S</i> ) <sup>[c]</sup>
3	<b>a</b> CO <sub>2</sub> Me	100 ( <i>S</i> )	CH <sub>2</sub> Cl <sub>2</sub>	25	2.5	78	93 ( <i>S</i> ) <sup>[c]</sup>
4	<b>a</b> CO <sub>2</sub> Me	10 ( <i>S</i> )	CH <sub>2</sub> Cl <sub>2</sub>	25	15	62	40 ( <i>S</i> ) <sup>[c]</sup>
5	<b>b</b> CO <sub>2</sub> Et	100 ( <i>S</i> )	CH <sub>2</sub> Cl <sub>2</sub>	0	3	70	92 ( <i>S</i> ) <sup>[c]</sup>
6	<b>c</b> phenyl	100 ( <i>S</i> )	CH <sub>2</sub> Cl <sub>2</sub>	25	72	0	–
7	<b>d</b> 1-naphthyl	100 ( <i>S</i> )	CH <sub>2</sub> Cl <sub>2</sub>	25	72	11	18 (n.d.) <sup>[d]</sup>
8	<b>e</b> 4-MeOPh	100 ( <i>R</i> )	CH <sub>2</sub> Cl <sub>2</sub>	25	72	0	–
9	<b>f</b> 2-furyl	100 ( <i>S</i> )	CH <sub>2</sub> Cl <sub>2</sub>	25	72	14	21 (n.d.) <sup>[d]</sup>
10	<b>f</b> 2-furyl	100 ( <i>R</i> )	toluene	25	72	0	–
11	<b>g</b> CH(OMe) <sub>2</sub>	10 ( <i>R</i> )	toluene	25	24	<9	n.d.
12	<b>g</b> CH(OMe) <sub>2</sub>	100 ( <i>R</i> )	toluene	25	18	59	67 ( <i>R</i> ) <sup>[e]</sup>
13	<b>g</b> CH(OMe) <sub>2</sub>	100 ( <i>R</i> )	toluene	0	15	19	65 ( <i>R</i> ) <sup>[e]</sup>
14	<b>g</b> CH(OMe) <sub>2</sub>	100 ( <i>R</i> )	CH <sub>2</sub> Cl <sub>2</sub>	25	18	25	39 ( <i>R</i> ) <sup>[e]</sup>
15	<b>g</b> CH(OMe) <sub>2</sub>	100 ( <i>R</i> )	THF	25	18	55	13 ( <i>R</i> ) <sup>[e]</sup>
16	<b>g</b> CH(OMe) <sub>2</sub>	100 ( <i>S</i> )	CH <sub>2</sub> Cl <sub>2</sub>	25	15	48	44 ( <i>S</i> ) <sup>[e]</sup>

[a] Isolated yield after silica gel chromatography. [b] Asymmetric induction determined by chiral HPLC. [c] Absolute stereochemistry determined by comparison of the HPLC with those reported in ref.<sup>[9]</sup>. [d] n.d. = not determined, due to low asymmetric induction or conversion. [e] Absolute stereochemistry determined by comparison of the CD curve vs. the DFT-calculated curve.

catalyst]. This result prompted us to examine this reaction further, and as with previous findings,<sup>[9]</sup> lowering the temperature did not have a positive impact upon the asymmetric induction (Entry 13), resulting in a very slight drop in the *ee* down to 65% at 0 °C and more sluggish reaction. More polar solvents (Entries 14 and 15) also had detrimental effects, which contrasts the ester-substituted systems **1a** and **b** (vide supra). Finally, use of (*S*)-binol (Entry 16) in dichloromethane gave a similar result to that obtained by using (*R*)-binol, but with reversal of the major enantiomer produced (compared to Entry 14).

### Assignment of Absolute Stereochemistry of Cycloadduct **3g**

In order to assign the absolute stereochemistry of the major enantiomer of the adduct **3g** shown in Entry 12 (Table 2), attempts were made to obtain suitable single crystals for X-ray analysis; however, all such attempts failed. Nevertheless, an excellent alternative was employed, i.e. by using the CD curve shown in Figure 2, which was recorded and compared with that obtained from TDDFT calculations.<sup>[15–17]</sup> Prior to this, the conformation of **3g** was investigated by means of experimental and computational methods. The <sup>1</sup>H NMR NOESY spectrum of **3g** was recorded to reveal major intramolecular proximity interactions and couplings, as shown in Figure 3. Molecular-mechanics conformational searches followed by DFT geometry optimisations resulted in a set of structures for **3g**, four of which (I–

IV) had population >5% at 298 K (Figure 4), the following ones having populations <2%. In all of these low-energy conformations, the dihydropyridinone ring assumes a sofa S(6) conformation<sup>[18]</sup> (with positive C3–C4–C5–C6 torsion for *R* absolute configuration), where the substituent at C-6 occupies a *pseudo*-axial position. The structures I–IV differ mainly in the conformation of the dimethoxyacetal moiety, additionally, I–III have negative phenyl–N–C2 dihedrals, while IV has a positive one; the key factor responsible for such a preference seems to be a C–H···O hydrogen bond<sup>[19]</sup> between an aromatic hydrogen and an acetal oxygen (dashed line in Figure 4). When low-energy DFT structures, in particular I, are checked against NMR spectroscopic

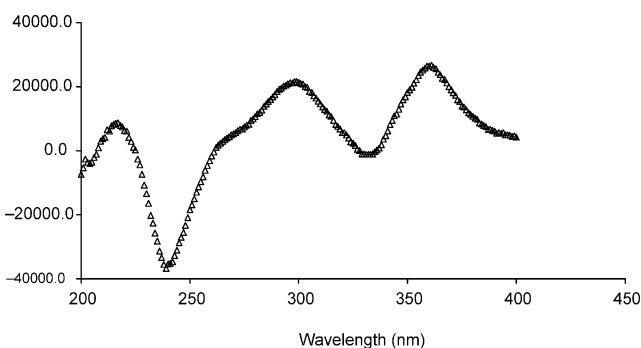


Figure 2. Observed CD curve for the dimethyl acetal cycloadduct **3g** derived the zinc(II)–(*R*)-binol complex (Table 2, Entry 12) (cell path length: 0.5 cm, solvent: MeCN).

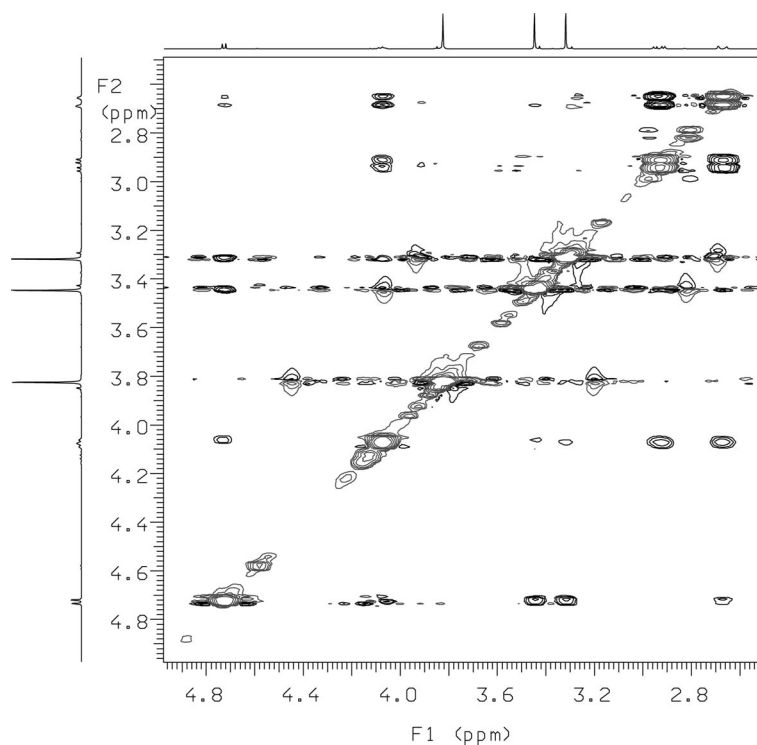


Figure 3. NOESY spectrum for dimethyl acetal cycloadduct **3g**, showing a clear NOE interaction between the signal at  $\delta = 2.68$  and 4.73 ppm (500 MHz, CDCl<sub>3</sub>).

data, the good agreement demonstrated by Figure 4 is found. The *pseudo*-axial position of the substituent at C-6 is proved by the NOE observed for the acetal hydrogen 7-H with the *cis*-related 5-H<sub>eq</sub>, but not with the *trans*-related 5-H<sub>ax</sub>. The value of 7.3 Hz measured for the *J* coupling between the acetal 7-H and the vicinal 6-H is also in keeping with an *anti* relationship as found in I (predicted value with the Haasnoot–de Leeuw–Altona equation, including all substituents at C-6 and C-7, is 8.5 Hz).<sup>[20]</sup>

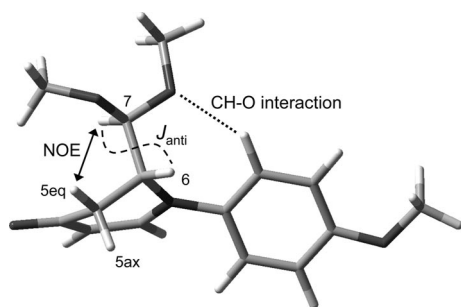


Figure 4. Lowest-energy DFT-computed structure (I) for **3g**, fitting diagnostic NMR spectroscopic data, plus relative energy and populations of other minima (II–IV) within 1.8 kcal/mol.

The CD spectra were calculated with TDDFT method for the four structures I–IV, then weighted according to Boltzmann distribution at 298 K and averaged (Figure 5). The average CD spectrum calculated for (*R*)-**3g** reproduces well the shape of the experimental spectrum (Figure 3), apart from a limited wavelength shift. Only the intensity of the first band around 350 nm is a little overestimated; this

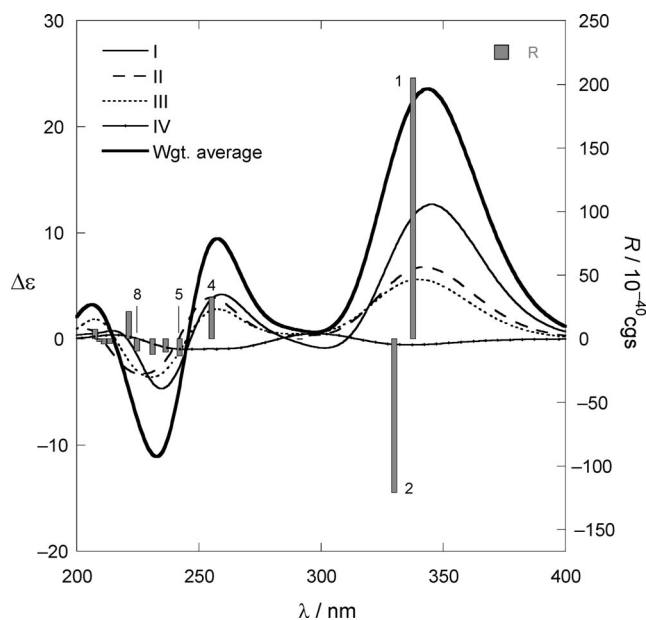


Figure 5. TDDFT-calculated CD curves for the low-energy conformations I–IV of (*R*)-**3g** (see Figure 4) weighted with respective Boltzmann factors at 298 K, and their sum spectrum. Vertical bars represent rotational strengths calculated for I.

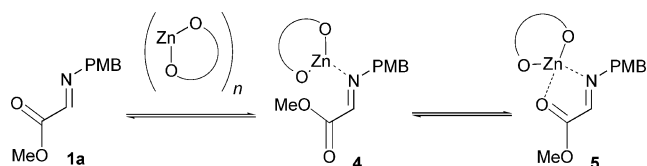
results from the superimposition of two transitions with opposite sign and very close in energy (#1–2 in Figure 5), so that a small adjustment of both intensities (say, –15% for #1 and +15% for #2) would be enough for a better match. These two bands arise from the combination of enone  $n-\pi^*$  and  $\pi-\pi^*$  excitations. The following transition (#4 in Figure 5) responsible for a positive CD band at 290 nm is similarly localised on the enone chromophore, while the next, negative CD at 240 nm is due to four different transitions (#5–8) also involving the aromatic ring.

The first three more stable structures I–III have comparable calculated CD curves, both in terms of shape and intensity, therefore, even a reasonable variation in their population (which cannot be checked experimentally) would not significantly affect the average spectrum. In conclusion, TDDFT CD calculations demonstrate that the application of zinc(II)–(*R*)-binol complex to the reaction of acetal-substituted imine **1g** with diene **2** results in the formation of the (*R*)-cycloadduct **3g**.

### Mechanism and Origin of Asymmetric Induction

Preliminary results on the effects of temperature and solvent from the zinc(II)–binol-catalysed formal cycloaddition of the ester-substituted imines **1a** and **b** with Danishefsky's diene **2** can be explained<sup>[9]</sup> in terms of at least two possible competing effects, i.e. firstly, the presence of a catalyst equilibrium between monomer and dimer complexes in solution; and secondly, that low catalyst are less effective due to the likelihood of competing silicon transfer effects.<sup>[9]</sup> However, these effects neither explain the sense of asymmetric induction as a function of catalyst absolute stereochemistry for the cycloaddition of the imines **1a** and **b**, nor the surprising reactivity of the acetal **1g** and the same sense of asymmetric induction compared with the imines **1a** and **b**. Because these types of aza-Diels–Alder cycloaddition reactions occur through a step-wise processes,<sup>[11]</sup> the imines **1** must be suitably activated for the initial Mannich-like addition step to proceed with the diene **2**. In Table 2, the unreactive or less reactive imines **1** are systems which are only monodentate zinc ligands, i.e. the aryl imines **1c–e**, with the exception being low reactivity furyl imine **1f**. The ester systems **1a** and **b**, and the dimethyl acetal system **1g** are all capable of being bidentate donor zinc ligands through their imine-nitrogen and carbonyl or acetal oxygen functions, respectively. Thus, in the case of the methyl ester imine **1a**, the proposed complexation equilibrium processes involved are described by Scheme 1 (complex **5** is also representative imine **1b**).

However, the furyl imine **1f** seems to be the exception at first sight, except that it also has the potential to provide act as a weak bidentate donor ligand through the furyl oxygen; a complex which is most favoured in the slightly more polar solvent, i.e. dichloromethane vs. toluene. This second chelation to zinc may be essential for reactivity of the imine **1f**, and such a weak oxygen–zinc complexation is expected to be dependent upon solvent polarity, presumably due to

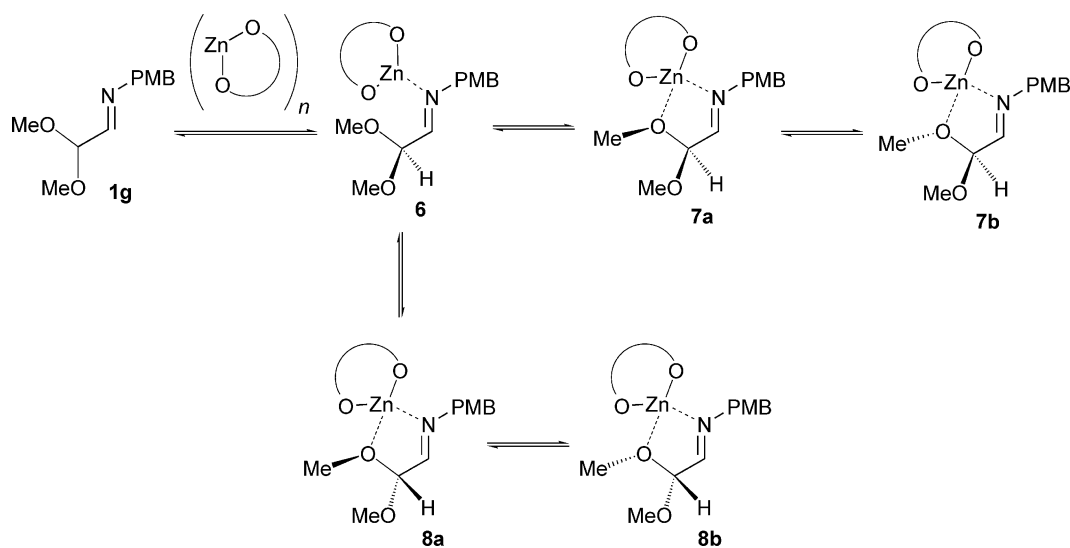


Scheme 1. Proposed mode of complexation of the imine **1a** by zinc(II)–binol.

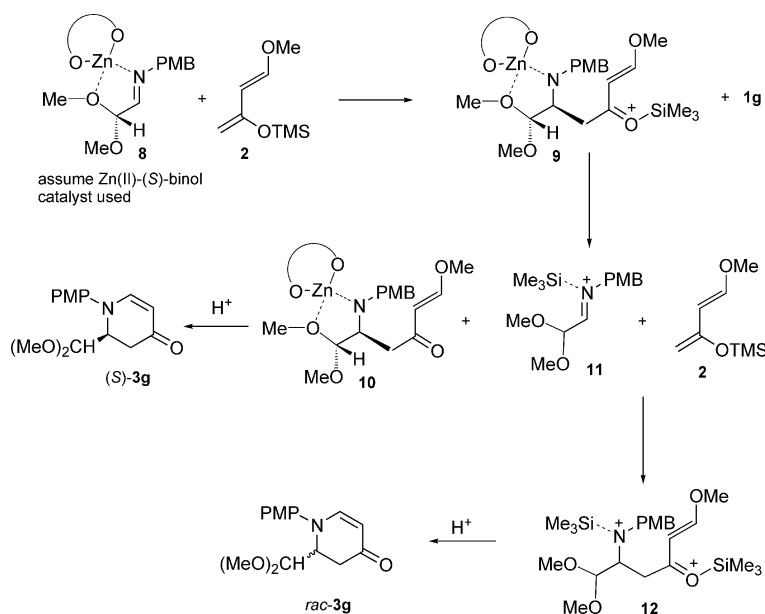
the competing zinc(II)–binol self-association (oligomerisation) discussed previously and elsewhere.<sup>[13b]</sup> In the case of the acetal-substituted imine **1g**, the complexes **7** and **8** (Scheme 2) are likely possibilities for explaining the surprising reactivity of this system. In the case of the imine **1g**, it is also interesting to note that the asymmetric induction

is somewhat lower, and the reactions slower, than for the corresponding ester-substituted imines **1a** and **b** (Table 2, Entries 1–5 vs. 11–16), and yet the complexes **5**, and **7** and **8** are clearly structurally similar.

Unsurprisingly, the ester-substituted systems **1a** and **b** are inherently more reactive than the corresponding acetal system **1g**, however, this does not explain the lower asymmetric induction for the acetal imine **1g**. A likely explanation stems from the competing slow, achiral silicon-transfer reaction<sup>[9]</sup> which can occur competitively. This process, explained in Scheme 3 and applied to imine **1g**, is enabled by the slow step-wise diene to imine addition, and a slow cyclisation process. This, the mechanism of addition of the diene **2b** to the imine **1g** is envisaged as occurring by the bidentate complex **8** (or **7**, *vide infra*) with addition of the



Scheme 2. Proposed modes of complexation of the imine **1g** by zinc(II)–binol.



Scheme 3. Proposed step-wise aza-Diels–Alder reaction of the imine **1g** with Danishefsky's diene involving both the zinc(II)–binol and competing silyl-transfer process.

diene-producing silyloxonium ion **9**. This species **9** can slowly cyclise, however, there is evidence for this being very slow, or only occurring upon acidic work up (yields of cyclic products in all these cycloaddition reactions are highly dependant upon work-up conditions, and the methods reported here have optimised to minimise the isolation of impure, unstable acyclic by-products). Alternatively, the species **9** can activate a further imine resulting in the silyl iminium ion **11**, which can react with the diene **2** to provide the racemic addition species **12**. Both complexes **10** and **12** will cyclise with suitable acidic work-up conditions, however, with diminished asymmetric induction (Scheme 3).

A further consequence of a proposed bidentate complexation of the imines **1** to zinc(II)–binol is that such relatively rigid complexes (such as **5**, **7**, and **8**) provide an opportunity for predictive molecular modelling. In the case of complexation of the acetal imine **1g** with zinc(II)–binol, the two acetal methoxy functions become diastereotopic, and hence, diastereoisomeric complexes **7** and **8** are likely to exhibit different levels of facial control during the addition of the diene (see Scheme 2), and further attention needs to be given to each of the diastereotopic oxygen lone pairs on each acetal oxygen (**7a** and **b**, and **8a** and **b**, Scheme 2). In the cases of the addition of diene **2** to the imines **1a**, **b** and **g**, the sense of asymmetric induction is the same, i.e. the (*S*)-binol-derived zinc(II) complex affords the (*S*)-cycloadducts **3a**, **b** and **g**. Molecular models and conformational distribution of the proposed imine complexes **5**, **7** and **8** were examined by a combination of molecular mechanics and semi-empirical methods resulting in the lowest energy structures shown in Figure 6 for complex **5**, and Figure 7 for each of the four zinc complexes **7** and **8** (in all cases, there were several higher energy complexes present with minor structural variations; all showed essentially the same facial blocking by the binol ligand system). All the structures shown in Figure 6 and 7 show that the *Si*-faces are much more accessible due one of the  $\alpha$ -CHs next to the binol oxygen projecting underneath the imine carbons. Complex **5** shows a major low-energy conformation with a relatively planar five-membered ring chelate in which there

is clear approach to the upper *Si*-face. The diastereoisomeric complexes **7** show the same CH projecting underneath the imine function, however, the lower energy complex **7b** lacks the axial acetal methyl function shown in **7a**. Approach of the diene to the top, *Si*, face of **7b** might be expected predominate due to lack of top-face repulsion from the upper methyl group in **7a**. For diastereoisomers **8**, they show the same binol ligand-derived lower face blocking to complexes **7**, and both complexes have similarly accessible upper imine (*Si*) faces, though they differ in stability by 4 kcal mol<sup>-1</sup>. Overall, it is the *Si*-face which is preferred for the imines **1a**, **b** and **1g** deriving the corresponding (*S*) adducts **3a**, **b** and **g** respectively when using the zinc(II)–(*S*)-binol complex, and these proposed models do support such an outcome.

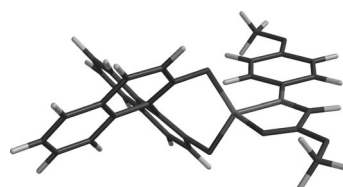


Figure 6. PM3-minimised molecular model of the lowest energy (–175 kcal mol<sup>-1</sup>) (*S*)-binol-derived zinc(II) complex **5** (this figure appears in colour as Figure S1 in the electronic supporting information).

## Conclusions

The zinc(II)–binol-mediated aza-Diels–Alder reaction of *N*-*p*-methoxyphenylimines with an electron-withdrawing ester function on the carbon is a reasonably efficient process, despite competing silicon-transfer-mediated processes.<sup>[9]</sup> In the present study, we have extended this work by employing zinc(II)–binol as Lewis acid catalyst (10 or 100 mol-% loading) for other related formal aza-Diels–Alder reactions, comparing the ester-substituted system with phenyl, naphthyl, furyl and dimethyl acetal-substituted imines. The

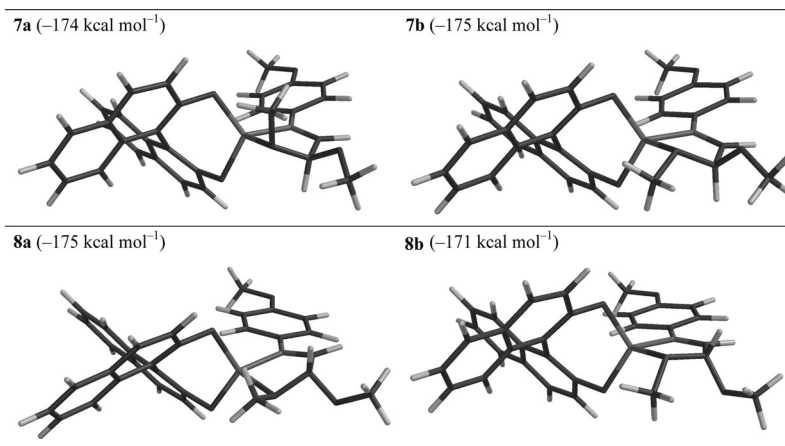


Figure 7. PM3-minimised molecular models of the lowest energy of each of the (*S*)-binol-derived zinc(II) complexes **7** and **8** (this figure appears in colour as Figure S2 in the electronic supporting information).

phenyl and naphthyl systems are oddly unreactive with zinc(II)–binol, the furyl imine has low reactivity which is highly solvent dependent, and the dimethyl acetal-substituted system is surprisingly reactive. The asymmetric induction in these types of reactions with Danishefsky's diene varies from poor to good depending on catalyst loading, solvent, temperature and substrate. However, the major enantiomer obtained is (*S*) when the (*S*)-binol complex has been employed in each case, and we have found that both efficient aza-Diels–Alder reaction and asymmetric induction are proposed to be dependent upon the formation of bidentate zinc-imine complexes. Further studies to optimise the catalytic asymmetric process and develop the applications of such asymmetric aza-Diels–Alder reactions are underway.

## Experimental Section

<sup>1</sup>H NMR spectra were recorded with Bruker AC200, AC250, AC300 and AC400 instruments and with Varian 200, 300 and 500 model spectrometers at frequencies of 200–500 MHz in [D]chloroform unless otherwise stated. <sup>13</sup>C NMR spectra were recorded on the same instruments at 50.3–125 MHz. <sup>1</sup>H and <sup>13</sup>C chemical shifts are expressed as parts per million downfield from the internal standard tetramethylsilane. EI (70 eV) and CI mass spectra were performed with Kratos MS25, Micromass Autospec or Finnigan MAT XP 95 spectrometers. ES mass spectra were recorded with Finnigan MAT 900 XLT and Micromass Autospec spectrometers. FAB spectra were recorded with a Kratos MS50 using *m*-nitrobenzyl alcohol matrix; high-resolution spectra were obtained from either Kratos Concept IS, Finnigan MAT 900 XLT or Micromass Autospec spectrometers. IR spectra were recorded with a Perkin–Elmer 298 spectrometer. HPLC were recorded using a Gilson HPLC system, with a UV detector set at 254 nm. Column chromatography was performed under medium pressure with Fluka silica gel (pore size 60 Å). Additional NMR spectra were measured with a Varian INOVA 600 spectrometer. All glassware used in anhydrous reactions was first dried with a heat-gun and cooled under a stream of argon. All extracted solvents were dried with MgSO<sub>4</sub> and evaporated at ca. 10–20 Torr using a Büchi rotary evaporator and water bath, followed by evaporation to dryness in vacuo. All solvents used were either distilled from sodium-benzophenone ketyl (THF) or calcium hydride (acetonitrile, DCM, petroleum ether, ethyl acetate and toluene) and stored under argon, or dried using a commercial drying system. All reagents used were purchased from Fluka, Lancaster Synthesis or Aldrich Chemical Co. and used as received, unless otherwise stated.

### Preparation of 2,2-Dimethoxyethylidene-4-methoxyaniline

**Procedure A:** Glyoxal dimethyl acetal (1.70 g, 16.4 mmol, 60% solution in water) was added to a solution of *p*-anisidine (2.01 g, 16.4 mmol) under argon in dichloromethane (80 mL), followed by anhydrous magnesium sulfate (ca. 20 g) until the reaction mixture appeared dry. Further *p*-anisidine (0.4992 g, 4.1 mmol) was added after 2 h, and the reaction mixture was stirred for a further 1.5 h. After the addition of charcoal (ca. 5 g), the mixture was filtered through Celite and evaporated to yield a crude dark brown oil (2.18 g, 51%).

**Procedure B:** Recrystallised *p*-anisidine (1.65 g, 0.013 mol) and magnesium sulfate (ca. 15 g) was added to a solution of glyoxal dimethyl acetal (1.39 g, 13 mmol, 60% solution in water) under ar-

gon in dichloromethane (60 mL) until the mixture appeared dry. After 2 h of stirring at room temperature the reaction mixture was filtered and the volatiles were evaporated to yield a crude yellow oil (2.64 g, 97%).

**Purification:** Crude imine (5.82 g) was distilled using a kugelrohr (180 °C, 1.3 Torr) to give pure imine (4.20 g, 87%): IR (thin film):  $\tilde{\nu}_{\max}$  = inter alia 1602 (C=N) cm<sup>-1</sup>. <sup>1</sup>H NMR (400 MHz, CDCl<sub>3</sub>):  $\delta$  = 3.46 (s, 6 H, 2 OCH<sub>3</sub>), 3.79 (s, 3 H, PhOCH<sub>3</sub>), 4.87 (d, *J* = 4.0 Hz, 1 H, CH-CH-N), 6.87 (d, *J* = 8.8 Hz, 2 H, ArH), 7.14 (d, *J* = 8.8 Hz, 2 H, ArH), 7.73 (d, *J* = 4.0 Hz, 1 H, CH-CH-N) ppm. <sup>13</sup>C NMR (100.6 MHz, CDCl<sub>3</sub>):  $\delta$  = 54.3 (2 OCH<sub>3</sub>), 55.7 (PhOCH<sub>3</sub>), 103.3 (H<sub>3</sub>COC), 114.5 (2 CH, aromatic), 122.5 (2 CH, aromatic), 143.4 (H<sub>3</sub>COCPh), 158.4 (HC=NCPH), 158.9 (HC=N) ppm. MS (ES+): *m/z* (%) = (inter alia) 210 (73) [M<sup>+</sup> + H], 124 (100) [C<sub>7</sub>H<sub>10</sub>NO]. Acc. MSC<sub>11</sub>H<sub>16</sub>NO<sub>3</sub> calcd. *m/z* 210.11247; found 210.11256.

**Preparation of Furylethylidene-4-methoxyaniline:** *p*-Methoxyaniline (0.56 g, 0.0046 mol) and dried magnesium sulfate (3.0 g) were added to a solution of 2-furaldehyde (0.44 g, 0.0046 mol) in dichloromethane (25 mL). This mixture was stirred at room temperature for 24 h after which time it was filtered and concentrated to give a brown oil (0.91 g) which solidified on standing. Recrystallisation from a CH<sub>2</sub>Cl<sub>2</sub>/hexane gave pure imine (0.71 g, 78%). M.p. 71–72 °C (ref.<sup>[13]</sup> 68–70 °C). IR (thin film):  $\tilde{\nu}_{\max}$  = (inter alia) 1610 (C=N) cm<sup>-1</sup>. <sup>13</sup>C NMR (100.6 MHz, CDCl<sub>3</sub>):  $\delta$  = 55.69 (OCH<sub>3</sub>), 112.39 (OCCHCH), 114.6 (OCCHCH), 115.89 (2 CH, aromatic), 122.54 (2 CH, aromatic), 144.4 (OCCH), 145.58 (OCCHCHCH), 145.95 (HC=N), 152.48 (OCH<sub>3</sub>CPh), 158.67 (HC=NCPH) ppm. All other spectroscopic and analytical data were as reported in the literature.<sup>[13]</sup>

**Aza-Diels–Alder Reaction of 2 with 2-Furylmethylidene-4-methoxyaniline (1f):** To a solution of ytterbium(III) triflate (0.062 g, 0.099 mmol) in dry acetonitrile under argon was added 2-furylmethylidene-4-methoxyaniline **1f** (0.200 g, 0.99 mmol). After 30 min, Danishefsky's diene **2** (0.40 mL, 1.99 mmol) was added and after a further 18 h, the reaction was quenched with aqueous hydrochloric acid (10 mL, 0.1 M). The mixture was extracted with dichloromethane, dried (MgSO<sub>4</sub>) and evaporated to give a dark oil. Purification by silica gel chromatography (petroleum ether/ethyl acetate, gradient elution) gave the adduct **3f**<sup>[13]</sup> as an orange solid (0.21 g, 76%). IR (thin film):  $\tilde{\nu}_{\max}$  = inter alia 1647 (CO), 1578 (C=C) cm<sup>-1</sup>. <sup>1</sup>H NMR (400 MHz, CDCl<sub>3</sub>):  $\delta$  = 2.85 (ddd, *HCH*, *J* = 16.5, 3.4 and 1.0 Hz, 1 H, 1 H), 3.12 (dd, *J* = 16.5 and 6.6 Hz, 1 H, *HCH*), 3.77 (s, 3 H, OCH<sub>3</sub>), 5.17–5.21 (m, 2 H, *HC-N-CH=CH*), 6.17 (d, *J* = 2.8 Hz, 1 H, O-CH=CH), 6.22 (dd, O-CH=CH, *J* = 2.8 and 1.6 Hz, 1 H, 1 H), 6.80 (d, *J* = 7.2 Hz, 2 H, ArH), 7.15 (d, *J* = 7.2 Hz, 2 H, ArH), 7.20–7.25 (m, 2 H, OCCHCHCH and NCH:CH) ppm. <sup>13</sup>C NMR (100.6 MHz, CDCl<sub>3</sub>):  $\delta$  = 40.2 (CH<sub>2</sub>), 55.8 (OCH<sub>3</sub>), 56.9 (CH<sub>2</sub>CH), 101.6 (NHC=CH), 108.8 (CH, furan), 110.6 (CH, furan), 114.9 (2 CH, aromatic), 122.1 (2 ArCH), 138.5 (O-CH-CH-CH), 142.8 (OCCH), 148.8 (NHC=HC), 151.2 (MeOCPh), 157.4 (NCPH), 190.8 (CO) ppm. MS (EI): *m/z* = 269 [M<sup>+</sup>], 175 (base peak) [M<sup>+</sup> – C<sub>6</sub>H<sub>4</sub>O]. Accurate MS (EI), calculated for C<sub>16</sub>H<sub>15</sub>NO<sub>3</sub>, 269.105194, found 269.105167.

**Aza-Diels–Alder Reaction of 2 with 2,2-Dimethoxyethylidene-4-methoxyaniline (1g):** 2,2-Dimethoxyethylidene-4-methoxyaniline **1g** (0.10 g, 0.475 mmol) was added to a solution of anhydrous magnesium(II) iodide (0.013 g, 0.0475 mmol) in dry acetonitrile under argon. After 30 min, Danishefsky's diene **2** (0.190 mL, 0.96 mmol) was added and after a further 48 h, the reaction was quenched with aqueous hydrochloric acid (10 mL, 0.1 M). The mixture was extracted with dichloromethane, dried (MgSO<sub>4</sub>) and evaporated to

give an orange oil (0.13 g). Purification by silica gel chromatography (petroleum ether/ethyl acetate, gradient elution) gave the adduct **3g** (0.11 g, 84%). IR (thin film):  $\tilde{\nu}_{\text{max}}$  = (inter alia) 1646 (CO)  $\text{cm}^{-1}$ .  $^1\text{H}$  NMR (400 MHz,  $\text{CDCl}_3$ ):  $\delta$  = 2.68 (br. d,  $J$  = 16.8 Hz, 1 H, *CHH*), 2.93 (dd,  $J$  = 16.8 and 6.7 Hz, 1 H, *CHH*), 3.32 and 3.45 (s, each 3 H, 2  $\text{CH-OCH}_3$ ), 3.83 (s, 3 H,  $\text{ArOCH}_3$ ), 4.07 (br. t,  $J$  = 7.0 Hz, 1 H,  $\text{CH}_2\text{CH}$ ), 4.73 (d,  $J$  = 7.3 Hz, 1 H, *CH-OMe*), 5.19 (d,  $J$  = 8.2 Hz, 1 H, *N-CH=CH*), 6.90 (d,  $J$  = 8.8 Hz, 2 H, *ArH*), 7.22 (d,  $J$  = 8.8 Hz, 2 H, *ArH*), 7.32 (d,  $J$  = 8.5 Hz, 1 H, *N-CH=CH*) ppm.  $^{13}\text{C}$  NMR (100.6 MHz,  $\text{CDCl}_3$ ):  $\delta$  = 36.9 ( $\text{CH}_2$ ), 56.3 (2  $\text{OCH}_3$ ), 56.4 ( $\text{PhOCH}_3$ ), 61.4 ( $\text{CH}_2\text{CH}$ ), 101.5 [ $(\text{CH}_3\text{O})_2\text{C}$ ], 102.2 (*NCHCH*), 114.9 (2  $\text{CH}$ , aromatic), 122.1 (2  $\text{CH}$ , aromatic), 139.07 ppm. MS (EI):  $m/z$  = 277 [ $\text{M}^+$ ], 216 (base peak) [ $\text{M}^+ - \text{C}_2\text{H}_5\text{O}_2$ ]. Accurate MS (EI), calculated for  $\text{C}_{15}\text{H}_{19}\text{NO}_4$  277.131408, found 277.131654.

#### General Procedure for the 10-mol-%-Catalysed Zinc(II)-(S)-Binol-Mediated Aza-Diels–Alder Reactions

**Example Methyl Ester 3a:** (*S*)-Binol (4.9 mg, 0.017 mmol) was dried under vacuum (1 h), dissolved in dry toluene (0.5 mL) under argon and treated with diethylzinc (15  $\mu\text{L}$  of a 1 M solution in hexanes). After 1 h, a solution of the imine **1a** (31 mg, 0.15 mmol) in toluene (1 mL) was added, followed by the diene **2** (43  $\mu\text{L}$ , 0.225 mmol) at the temperature indicated in Table 2. After completion (Table 2), the reaction mixture was hydrolysed with aqueous hydrochloric acid (1%, 2 mL), separated, washed with water, dried ( $\text{MgSO}_4$ ) and the solvents evaporated. Purification by silica gel chromatography (hexanes/ $\text{EtOAc}$ , 1:1, as eluent) gave adduct **3a** (Table 2).

The *ee* values for **3a** were determined by chiral HPLC using a Daicel Chiralcel OD column: eluent, hexane/IPA, 70:30; flowrate, 1.0 mL/min. Retention times: (*R*), 17.2 min; (*S*), 25.6 min.

**Aza-Diels–Alder Reaction of 2 with 2,2-Dimethoxyethylidene-4-methoxyaniline (1g) Catalysed by Stoichiometric Zinc(II)-(R)-Binol:** (*R*)-Binol (275 mg, 0.96 mmol) was dried under vacuum, dissolved in dry toluene (3.2 mL) under argon, forming a milky white suspension, and treated with diethylzinc (970  $\mu\text{L}$  of a 1 M solution in hexane). After 1 h, a solution of 2,2-dimethoxyethylidene-4-methoxyaniline **1g** (197 mg, 0.94 mmol) in dry toluene (4 mL) was added, followed by Danishefsky's diene **2** (227  $\mu\text{L}$ , 1.45 mmol). The reaction mixture was left stirring at room temperature for 18 h, after which the reaction was complete. The reaction was then quenched with hydrochloric acid (5%, 5 mL), and the colour of the mixture turned dark black. The layers were separated, with the aqueous layer being extracted with toluene ( $3 \times 10$  mL). All the organic layers were then combined, washed with brine (30 mL), dried ( $\text{MgSO}_4$ ), and the solvents evaporated. Purification by silica gel chromatography (hexane/ethyl acetate, 2:8, as eluent) gave the adduct **3g** in 67% *ee* (0.147 g, 59%).  $[\alpha]_{\text{D}}^{21} = +0.65$  ( $c$  = 0.4 MeCN). All spectroscopic analytical properties were identical to those reported above.

The *ee* values for **3g** were determined by chiral HPLC using a Daicel Chiralcel OD column: eluent, hexane/IPA, 75:25; flowrate, 1.0 mL/min. Retention times: (*S*) 13.55 min; (*R*) 20.15 min.

**X-ray Crystallography:** X-ray diffraction experiment was carried out with a Bruker 3-circle diffractometer with a SMART 6 K CCD area detector, using graphite-monochromated  $\text{Mo-K}\alpha$  radiation ( $\lambda$  = 0.71073 Å) and a Cryostream (Oxford Cryosystems) open-flow  $\text{N}_2$  cryostat. The structure was solved by direct methods and refined by full-matrix least-squares against  $F^2$  of all reflections, using SHELXTL software (version 6.12, Bruker AXS, Madison WI, USA, 2001).

**Crystal Data for 3f:**  $\text{C}_{16}\text{H}_{15}\text{NO}_3$ ,  $M$  = 269.29,  $T$  = 120 K, orthorhombic, space group  $P2_12_12_1$  (No. 19),  $a$  = 5.244(1),  $b$  = 14.602(3),  $c$  = 16.980(3) Å,  $U$  = 1300.2(5) Å<sup>3</sup>,  $Z$  = 4,  $D_{\text{calcd.}}$  = 1.376  $\text{g}/\text{cm}^{-3}$ ,  $\mu$  = 0.10  $\text{mm}^{-1}$ , 9396 reflections with  $2\theta \leq 54.5^\circ$ ,  $R$  = 0.032 on 1362 data with  $I \geq 2\sigma(I)$ ,  $wR(F^2)$  = 0.073 on all 1711 unique data (1197 Friedel pairs merged,  $R_{\text{int}}$  = 0.048).

CCDC-B706630A contains the supplementary crystallographic data for this paper. These data can be obtained free of charge from the Cambridge Crystallographic Data Centre via [www.ccdc.cam.ac.uk/data\\_request/cif](http://www.ccdc.cam.ac.uk/data_request/cif).

#### Computational Section

**CD Spectra:** Conformational searches were run employing Molecular Merck force field (MMFF), with standard parameters and convergence criteria, implemented in Spartan'06, Wavefunction, Inc, Irvine, CA, USA. All minima thus found were optimised with DFT, B3LYP/6-31G(d) level,<sup>[21]</sup> using Gaussian'03W, Revision B.05, Gaussian, Inc, Pittsburgh, PA, USA. TDDFT calculations were run with G03W on all minima within 1.8 kcal/mol, employing the hybrid functional B3LYP and the triple- $\zeta$  basis set with polarisation functions TZVP.<sup>[7]</sup> The first eight computed transitions involved virtual orbitals with negative eigenvalues and had energies below the estimated ionisation potential.<sup>[22]</sup> CD spectra were generated by applying a Gaussian band-shape with 4200  $\text{cm}^{-1}$  half-height width (corresponding to 50 nm at 350 nm) to rotational strengths computed with the dipole-length gauge formulation; rotational strengths computed for most transitions with dipole-velocity gauge formulation differed from dipole-length values by less than 5%.

**Zinc(II)-(S)-Binol Complexes:** Each of the likely zinc(II)-(S)-binol-imine complexes were built and subjected to conformational searches were run employing Molecular Merck force field (MMFF), with standard parameters and convergence criteria, and all minima thus found were optimised using the PM3 semi-empirical method,<sup>[23]</sup> as implemented in Spartan'04, Wavefunction, Inc., Irvine, CA, USA.

**Supporting Information** (see also the footnote on the first page of this article): Figure S1. PM3-minimised molecular model of the lowest energy ( $-175$  kcal  $\text{mol}^{-1}$ ) (*S*)-binol-derived zinc(II) complex **5** (colour) and Figure S2. PM3-Minimised molecular models of the lowest energy of each of the (*S*)-binol-derived zinc(II) complexes **7** and **8** (colour).

#### Acknowledgments

We thank the Engineering and Physical Sciences Research Council (EPSRC) for funding (reference number GR/N36066/01) and to the EPSRC mass spectrometry service at the University of Wales, Swansea.

- [1] a) G. M. Strunzand, J. A. Findlay, *The Alkaloids* (Ed.: A. Brossi), Academic Press, San Diego, **1986**, vol. 26; A. D. Elbein, R. Molyneux, *Alkaloids; Chemical and Biological Properties* (Ed.: S. W. Pelletier), John Wiley & Sons, New York, **1987**, vol. 57.
- [2] V. H. Lillelund, H. H. Jensen, X. Liang, M. Bols, *Chem. Rev.* **2002**, *102*, 515–553.
- [3] a) P. Buonora, J.-C. Olsen, T. Oh, *Tetrahedron* **2001**, *57*, 6099–6138; b) D. Boger, S. M. Weinreb, *Hetero Diels–Alder Methodology in Organic Synthesis*, Academic Press, San Diego, **1987**, chapter 2, pp. 34–70.
- [4] K. A. Jørgensen, *Angew. Chem. Int. Ed.* **2000**, *39*, 3558–3588.
- [5] a) S. Yao, M. Johannsen, R. G. Hazell, K. A. Jørgensen, *Angew. Chem. Int. Ed. Engl.* **1998**, *37*, 3121–3124; b) S. Yao, S.

- Saaby, R. G. Hazell, K. A. Jørgensen, *Chem. Eur. J.* **2000**, *6*, 2435–2448; c) S. Kobayashi, S. Komiyama, H. Ishitani, *Angew. Chem. Int. Ed. Engl.* **1998**, *37*, 979–981; d) H. Ishitani, M. Ueno, S. Kobayashi, *J. Am. Chem. Soc.* **1997**, *119*, 7153–7154; e) S. Kobayashi, K. Kusakabe, S. Komiyama, H. Ishitani, *J. Org. Chem.* **1999**, *64*, 4220–4221; f) S. Kobayashi, K. Kusakabe, H. Ishitani, *Org. Lett.* **2000**, *2*, 1225–1227; g) N. S. Josephsohn, M. L. Snapper, A. H. Hoveyda, *J. Am. Chem. Soc.* **2003**, *125*, 4018–4019.
- [6] a) S. Bromidge, P. C. Wilson, A. Whiting, *Tetrahedron Lett.* **1998**, *39*, 8905–8908; b) A. Bundu, S. Guillarme, J. Hannan, H. Wan, A. Whiting, *Tetrahedron Lett.* **2003**, *44*, 7849–7850.
- [7] a) O. Corminboeuf, P. Renaud, *Org. Lett.* **2002**, *4*, 1735–1738; b) O. G. Mancheño, R. G. Arrayás, J. C. Carretero, *J. Am. Chem. Soc.* **2004**, *126*, 456–457; c) T. Akiyama, Y. Tamura, J. Itoh, H. Morita, K. Fuchibe, *Synlett* **2006**, 141–143.
- [8] H. Du, J. Long, J. Hu, X. Li, K. Ding, *Org. Lett.* **2002**, *4*, 4349–4352.
- [9] S. Guillarme, A. Whiting, *Synlett* **2004**, 711–713.
- [10] S. J. Danishefsky, T. Kitahara, *J. Am. Chem. Soc.* **1974**, *96*, 7807.
- [11] a) S. Hermitage, D. J. Jay, A. Whiting, *Tetrahedron Lett.* **2002**, *43*, 9633–9636; b) S. Hermitage, J. A. K. Howard, D. Jay, R. G. Pritchard, M. R. Probert, A. Whiting, *Org. Biomol. Chem.* **2004**, *2*, 2451–2460.
- [12] I. Ojima, I. Habus, M. Zhao, M. Zucco, Y. H. Park, C. M. Sun, T. Brigaud, *Tetrahedron* **1992**, *48*, 6985–7012.
- [13] a) T. Akiyama, K. Matsuda, K. Fuchibe, *Synlett* **2002**, 1898–1900; b) Y. Yuan, X. Li, K. Ding, *Org. Lett.* **2002**, *4*, 3309–3311; c) Y. Yuan, X. Li, K. Ding, *Org. Biomol. Chem.* **2005**, *3*, 239–244; d) C. Loncaric, K. Manabe, S. Kobayashi, *Chem. Commun.* **2003**, 574–575.
- [14] a) B. Alcaide, P. Almendros, J. M. Alfonso, M. F. Aly, M. R. Torres, *Synlett* **2001**, 1531–1534; b) B. Alcaide, P. Almendros, J. M. Alfonso, M. F. Aly, *Chem. Eur. J.* **2003**, *9*, 3415–3426.
- [15] a) A. Dreuw, M. Head-Gordon, *Chem. Rev. (Washington, DC, U. S.)* **2005**, *105*, 4009–4037; b) M. A. L. Marques, E. K. U. Gross, *A Primer in Density Functional Theory in Lecture Notes in Physics, Time-Dependent Density Functional Theory* (Eds.: C. Fiolhais, F. Nogueira, M. A. L. Marques), vol. 620, Springer, Berlin **2003**, pp. 144–184.
- [16] a) T. D. Crawford, *Theor. Chem. Acc.* **2006**, *115*, 227–245; b) C. Diedrich, S. Grimme, *J. Phys. Chem. A* **2003**, *107*, 2524–2539.
- [17] a) L. Di Bari, G. Pescitelli, P. Salvadori, M. Rovini, M. Anzini, A. Cappelli, S. Vomero, *Tetrahedron: Asymmetry* **2006**, *17*, 3430–3436; b) H. Hussain, K. Krohn, U. Flörke, B. Schulz, S. Draeger, G. Pescitelli, S. Antus, T. Kurtán, *Eur. J. Org. Chem.* **2007**, 292–295; c) K. Krohn, I. Kock, B. Elsässer, U. Flörke, B. Schulz, S. Draeger, G. Pescitelli, S. Antus, T. Kurtán, *Eur. J. Org. Chem.* **2007**, 1123–1129; d) A. Krick, S. Kehraus, C. Gerhäuser, K. Klimo, M. Nieger, A. Maier, H. H. Fiebig, I. Atodiresei, G. Raabe, J. Fleischhauer, G. M. König, *J. Nat. Prod.* **2007**, *70*, 353–360; e) K. Krohn, Zia-Ullah, U. Flörke, B. Schulz, S. Draeger, G. Pescitelli, P. Salvadori, S. Antus, T. Kurtán, *Chirality*, **2007**, in press; f) K. Krohn, U. Farooq, U. Flörke, B. Schulz, S. Draeger, G. Pescitelli, P. Salvadori, S. Antus, T. Kurtán, *Eur. J. Org. Chem.* **2007**, in press.
- [18] J. Gawronski, *Conformations, Chiroptical and Related Spectral Properties of Enones in The Chemistry of Enones* (Eds. S. Patai, Z. Rappoport), Wiley, Chichester, **1989**, chapter 3, pp. 55–105.
- [19] a) G. R. Desiraju, *Acc. Chem. Res.* **1996**, *29*, 441–449; b) U. Koch, P. L. A. Popelier, *J. Phys. Chem.* **1995**, *99*, 9747–9754.
- [20] C. Altona in *Encyclopedia of NMR* (Eds. D. M. Grant, R. Morris), Wiley, New York, **1996**, pp. 4909–4923.
- [21] See Gaussian'03 documentation at [http://www.gaussian.com/g\\_ur/g03mantop.htm](http://www.gaussian.com/g_ur/g03mantop.htm) for details on basis sets and DFT functionals.
- [22] M. E. Casida, C. Jamorski, K. C. Casida, D. R. Salahub, *J. Chem. Phys.* **1998**, *108*, 4439–4449.
- [23] J. J. P. Stewart, *J. Comput. Chem.* **1989**, *10*, 209–220.

Received: August 3, 2007

Published Online: October 2, 2007